Review paper: The 30th March 1968 M_w 5.7 Marryat Creek surface rupturing earthquake, Australia

Tamarah King

School of Earth Sciences, The University of Melbourne, Victoria 3010, Australia
tamarah.king@unimelb.edu.au
https://orcid.org/0000-0002-9654-2917

Mark Quigley

School of Earth Sciences, The University of Melbourne, Victoria 3010, Australia
Mark.quigley@unimelb.edu.au
https://orcid.org/0000-0002-4430-4212

Dan Clark

Geoscience Australia, Canberra 2601, Australia
https://orcid.org/0000-0001-5387-4404

Abstract

The 30th March 1986 M_w 5.7 Marryat Creek earthquake produced a highly arcuate 13 km long surface rupture with maximum vertical displacement of 0.9 m. Sinistral displacement on the NE-SW limb, dextral displacement on the NNE-SSW limb, and maximum vertical displacement in the central apex of rupture supports SW over NE movement of a hanging-wall block. Epicentre locations are poorly constrained and inaccurate, locally exceeding distances of 30 km from the surface rupture. The most geologically and seismologically reasonable fault rupture model involves 3 bedrock-controlled faults. Assuming simple planar geometry, these would intersect 5.5 km SW of the rupture at 3 km depth, which is consistent with centroid depths of 3 – 4.5 km. Two trenches across the 1986 rupture trace show no preceding discrete offset since deposition of overlying sediments (100 – 130 ka). Strong evidence exists to suggest historic surface rupture was controlled by basement structures including a large pre-existing fault, but only circumstantial evidence supports any prior neotectonic rupture. This earthquake is one of the most structurally complex (as proxied by the number of discrete faults) for its magnitude, as evidenced by comparison with a global compilation.

This document presents a review of available literature related to the 1986 Marryat Creek surface rupturing earthquake. It includes newly digitised data related to the rupture and new interpretations of controls on fault rupture. It supplements a manuscript reviewing all Australian surface rupturing earthquakes, submitted to Geosciences in August 2019.

Please contact authors on the content presented herein; we welcome constructive feedback.

---

1. Geology

1.1 Regional / background

The 1986 Marryat Creek, 2012 Pukatja and 2016 surface rupturing earthquakes occurred within the Musgrave Block, a Mesoproterozoic basement assemblage that extends across the Northern Territory / South Australia into Western Australia (Figure 1). This block is composed of high grade metamorphic and magmatic suites formed during the ~1200 Ma Musgrave orogen and reworked during the 580 - 520 Ma Petermann Orogeny (Aitken and Betts, 2009; Cawood and Korsch, 2008; Edgoose et al., 2004; Raimondo et al., 2010). Two large structures, the Woodroffe Thrust and Mann Fault, dominated uplift and deformation during the Petermann Orogeny (Lambeck and Burgess, 1992; Neumann, 2013; Stewart, 1995; Wex et al., 2019). The Woodroffe Thrust was responsible for significant exhumation of lower-crustal rocks, displacing the Moho by ~20 km associated with a present-day large gravitational and magnetic anomaly (Hand and Sandiford, 1999; Korsch et al., 1998; Wade et al., 2008). The Petermann and Pukatja surface ruptures occurred within 10 km of the Woodroffe Thrust (on the hanging-wall), and the Marryat Creek rupture is coincident with the location of the Mann Thrust as mapped by some authors (Aitken and Betts, 2009; Raimondo et al., 2010).

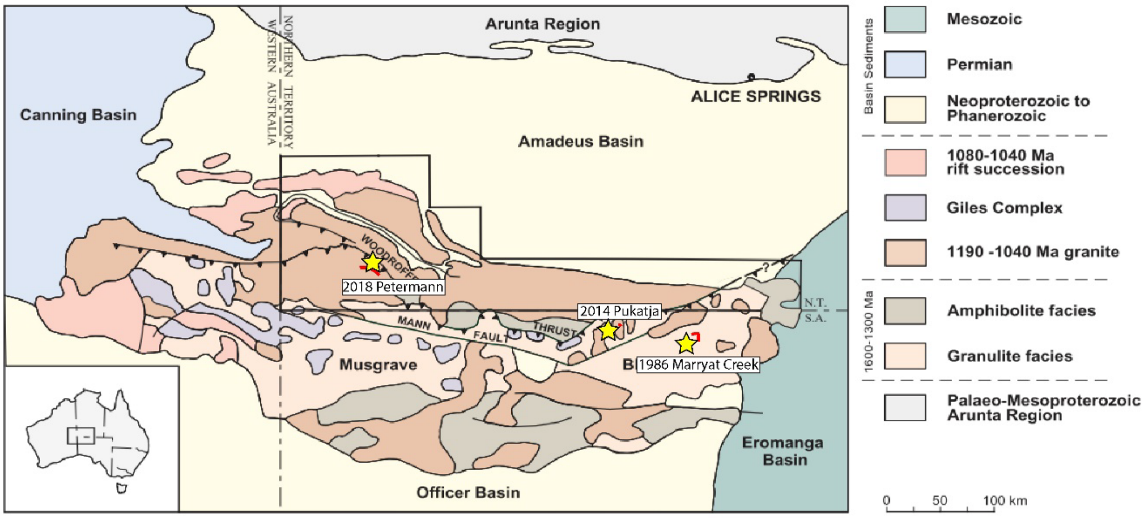

Figure 1: Musgrave Block geology from Figure 3 of Edgoose et al. (2004) with Petermann, Pukatja and Marryat Creek earthquakes (yellow stars) and ruptures (red lines) overlaid. Note some authors locate the Mann Fault further south than this map, coincident with the location of the Marryat Creek rupture (Aitken and Betts, 2009; Raimondo et al., 2010). *(CC) NT Gov*

1.2 Local bedrock

The Marryat Creek surface rupture occurred in an area where near-surface granitic metamorphic rocks are cross-cut by faults and dikes. The NE-SW limb of rupture (herein termed MC_1) is coincident with the location of the Mann fault as mapped by some authors (Aitken and Betts, 2009; Raimondo et al., 2010) visible as a linear magnetic anomaly striking east-west (Figure 3). Bedrock close to the surface rupture (0 - 5 km) occurs as low-lying isolated outcrops and is described as altered and deformed metamorphosed granite (Machette et al., 1993) (Figure 2, Figure 4). Dikes are mapped on the 1 : 250 000 geological map (Fairclough et al., 2011) and described by some authors investigating the historic surface rupture (Machette et al., 1993) within 5 km of the surface rupture in either a roughly NE-SW or NW-SE orientation (Figure 4). Bedrock outcrops visible on satellite imagery close to the surface rupture have three sets of structural / intrusive orientations matching the three main strike directions of the historic surface rupture (Figure 2, Figure 4). Small outcrops of gneissic bedrock are exposed in the hanging-wall adjacent to the Marryat Creek North trench site described in Machette et al. (1993).

The authors find that foot-wall bedrock is heavily sheared and altered in their trench (Section 4.2), which they attribute to a pre-existing fault.

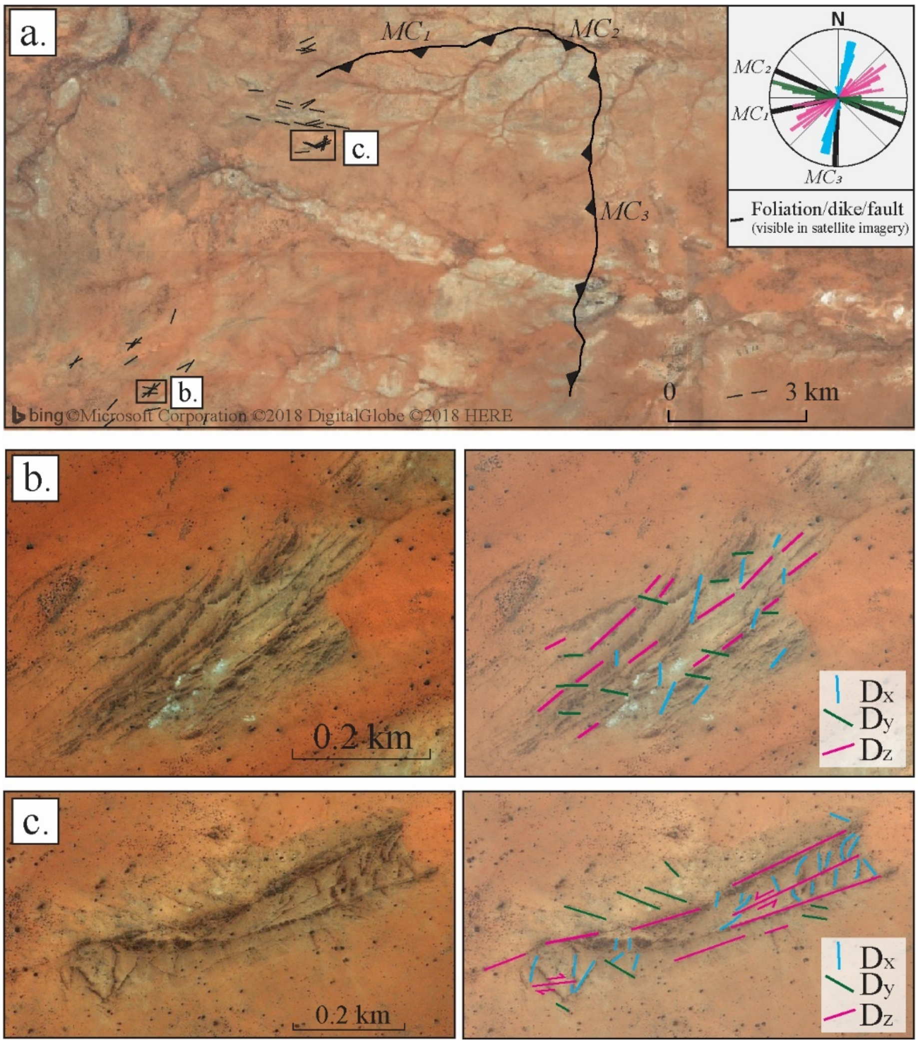

Figure 2: Satellite imagery (Bing © 2019 DigitalGlobe, HERE, Microsoft) of outcrops close to the Marryat Creek rupture showing three clear sets of structural orientations

The MC_1 limb of the arcuate Marryat Creek scarp overlies and aligns with a linear magnetic anomaly that displaces other north-south trending magnetic anomalies. This limb is also sub-parallel to a large ~ 280 km long regional gravity anomaly (Figure 3). This anomaly is mapped by some authors as the Mann Fault, a structure that extends across the Musgrave Block (Aitken and Betts, 2009; Raimondo et al., 2010). The NNE-SSW limb of rupture (herein termed MC_3) is sub-parallel to pervasive NNE-SSW fabrics apparent on the magnetic anomaly map. Multiple WNW-ESE linear anomalies are also visible, aligning with the central section of the surface rupture (herein termed MC_2). The coincidence between all three sections of surface rupture with bedrock orientations visible at the surface (Figure 2), and as pervasive linear magnetic anomalies (Figure 3) suggests that rupture was controlled by pre-existing structures within the deformed and metamorphosed granitic basement (e.g. dikes, foliation, faults). This is supported by trenching conducted across the rupture (see Section 10).

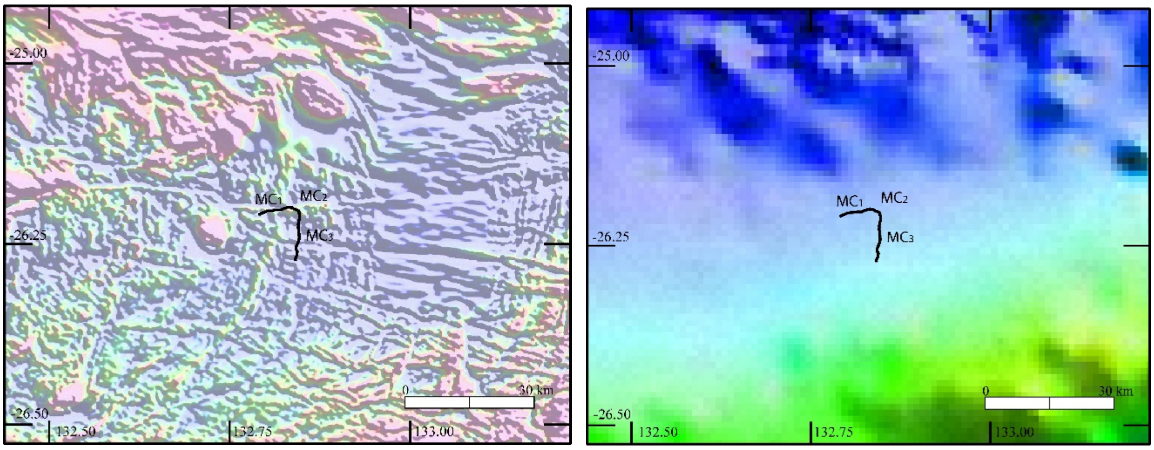

Figure 3: Marryat Creek scarp (black lines) relative to magnetic anomaly and bouguer gravity anomaly maps. National bouguer gravity anomaly map: [http://pid.geoscience.gov.au/dataset/ga/101104.](http://pid.geoscience.gov.au/dataset/ga/101104) National total magnetic intensity map: http://pid.geoscience.gov.au/dataset/ga/89596

1.3 Surficial deposits

Bedrock is overlain by clastic alluvial, colluvial and aeolian sediments and soils (Figure 4) up to 10 m thick in dunes and drainages , but generally < 3 m thick and underlain by gneissic or granulite basement (as logged in water bore-hole data[1] surrounding the surface rupture at < 15 km distance).

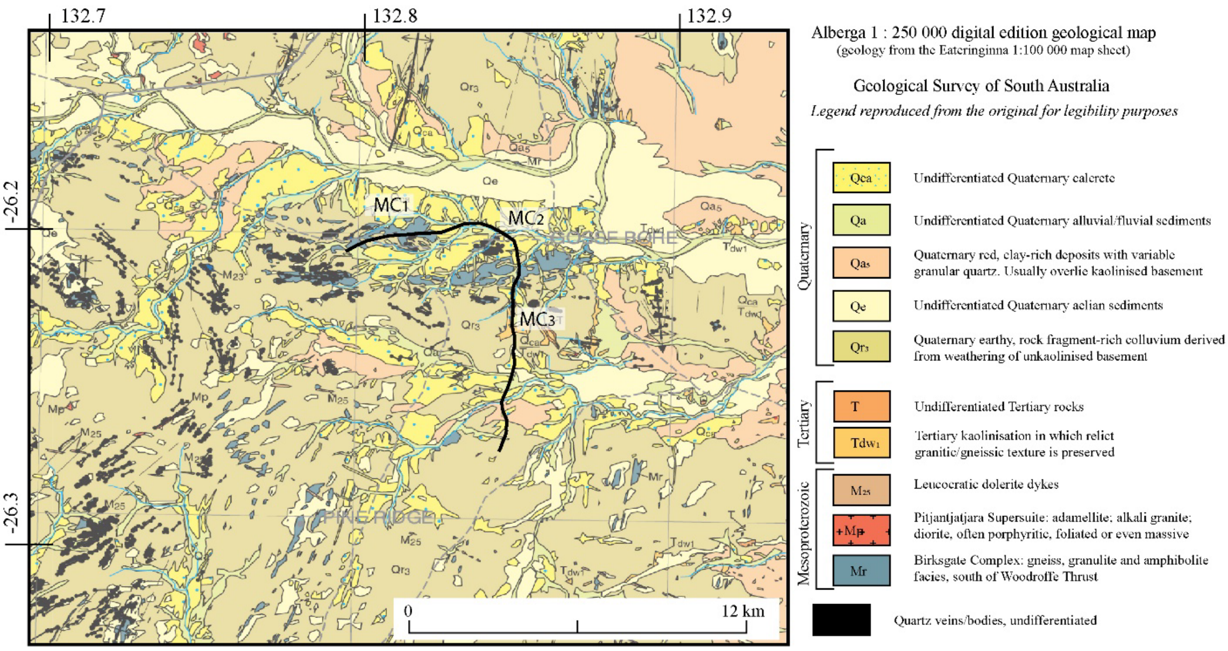

Figure 4: Crop of Alberga 1:250 000 digital edition geological map sheet (Fairclough et al., 2011) showing basement and surface sediments around the Marryat Creek surface rupture. Full map and legend available from Government of South Australia, Department for Energy and Mining: http://www.energymining.sa.gov.au/minerals/online_tools/free_data_delivery_and_publication_downloads/digital_maps_and_data

[1] https://www.waterconnect.sa.gov.au/Systems/GD/Pages/Default.aspx

2. Seismology

2.1 Epicentre and magnitude

The Marryat Creek earthquake occurred more than 300 km from the nearest seismometer (Alice Springs). Some instrumental recordings were omitted from epicentral determinations due to high negative travel time residuals (between 5 – 17 degrees) (Barlow et al., 1986). The first published locations (Barlow et al., 1986) for the USGS place the epicentre ~ 15 km SW of the surface rupture, and for GA (then BMR) ~35 km SW of the rupture (this location is the current GA epicentre in the online catalogue). A revised location was published by McCue et al. (1987) ~ 5 km west of the surface rupture on the hanging-wall, but they do not elaborate on how this revision was made (it is assumed they located it relative to the surface rupture hanging-wall). Denham (1988) provide updated locations from the USGS, GA and one based on the surface rupture location. The recently published NSHA18 catalogue (Allen et al., 2018) places the epicentre ~ 15 km south-west of the rupture, it is unknown how this location was derived. The GA, USGS and NSHA18 epicentres do not lie close enough to the surface rupture location to be considered accurate. The only published uncertainty values are in the GA_online catalogue (± 1 km), and are considered lower that what is reasonable given the instrumental density (statistical uncertainties are considered to be closer to ± 10 km (Leonard, 2008)). The mis-location of seismological epicentres away from the surface rupture is a considered to be a combination of the velocity model used by each agency, and other epistemic uncertainties. These large epistemic uncertainties in epicentre location also affected foreshock and aftershock distributions (discussed below).

This paper prefers the magnitude (M_W 5.7) of the recently published NSHA18 catalogue (Allen et al., 2018) as they conduct a thorough and consistent reanalysis of Australian magnitude values, particularly to address inconsistencies in the determination of historic magnitude values. This is generally consistent with previously reported magnitude values (M_L/M_b/M_s 5.7 - 5.8).

Table 1 : Published epicentre locations, depths and magnitudes

Reference	Agency	Latitude	± (km)	Longitude	± (km)	Depth (km)	± (km)	M1	M2
GA_online	GA	-26.333	1	132.517	1	5		5.7 Mw	6 M_L
Barlow et al (1986)	GA	-26.33		132.52		0			
McCue et al (1987)	Rupture based	-26.22		132.82				5.7 Mb	5.8 Ms,
Allen et al (2018)		-26.31		132.734		5		5.7 Mw	
Barlow et al (1986)	Rupture based	-26.199		132.83					
Barlow et al (1986)	"South Australia"	-26.285		133.019		19		5.2 M_L	
Barlow et al (1986)	USGS	-26.23		132.7		10		5.8 Ms	5.7 Mb
Denham (1988)	Rupture based	-26.2		132.8				5.8 Ms	

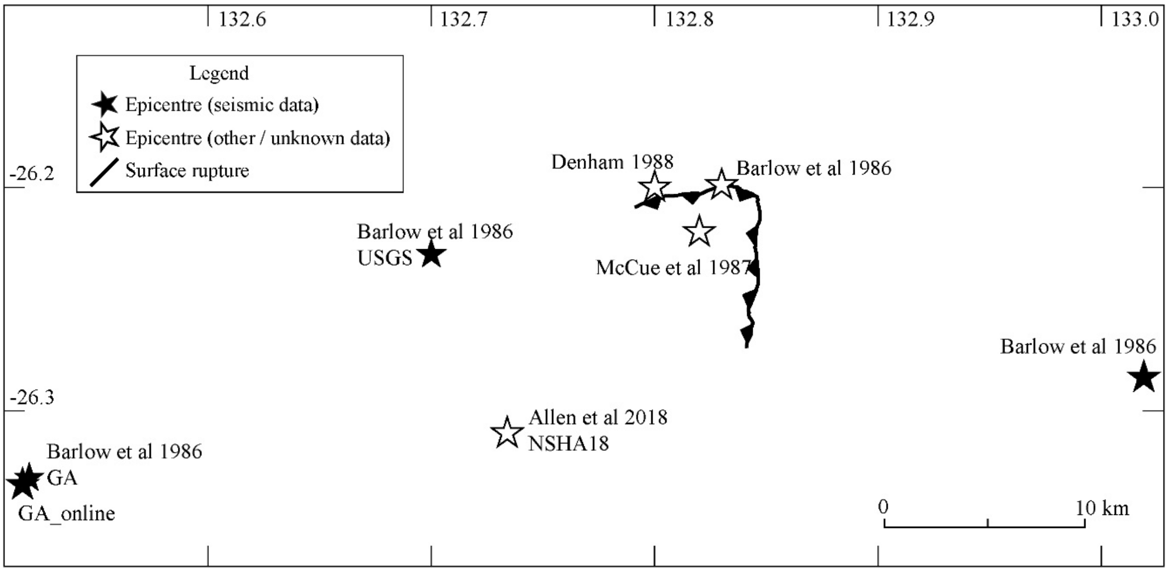

Figure 5: Published epicentre locations around the surface rupture.

2.2 Focal mechanisms

Three focal mechanisms are published for the Marryat Creek event; Barlow et al. (1986) (reproduced in (McCue et al., 1987)), Fredrich et al. (1988), and Global CMT (Ekström et al., 2012) (*Figure 6*). The Barlow et al. (1986) solution uses P-wave first motions and suggests a largely strike-slip component to movement, with the strike of either plane matching the trace of either limb of the surface rupture (which is highly arcuate). McCue et al. (1987) prefer the E-W plane of this solution which implies a sinistral movement on a steep 67° S dipping fault. Fredrich et al.(1988) invert teleseismic long- and short period P-waves, and long period SH-waves to derive their solution with an uncertainty of ± 20° on their focal mechanism strike. The arcuate surface rupture shows an overall west over east movement, and the west dipping CMT and Fredrich et al.(1988) solutions give a slightly dextral component of movement along a 35 - 42° SW dipping fault. A potential way to reconcile these focal mechanism solutions is a scenario where P-wave first motions represent an initial sub-event on a steep south or west dipping plane (e.g. MC_1 / MC_3), prior to the mainshock on a shallower SW dipping fault (e.g. MC_1) as recorded by teleseismic body-waves.

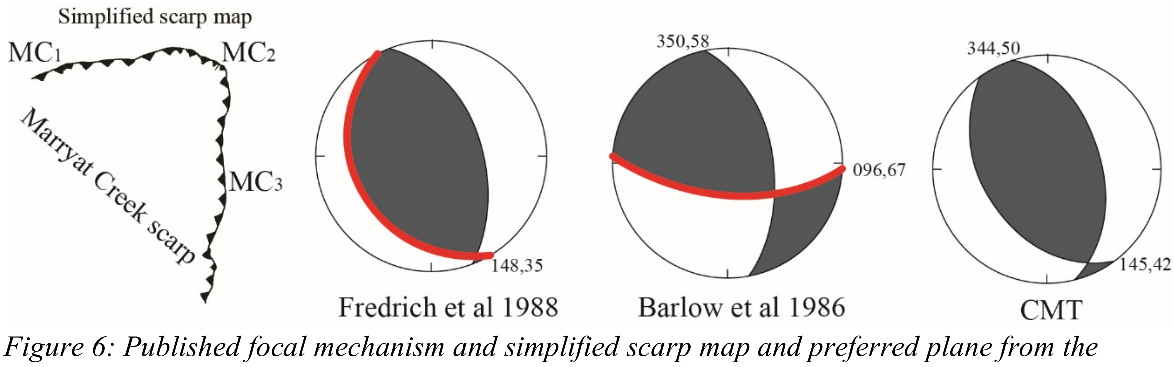

Figure 6: Published focal mechanism and simplified scarp map and preferred plane from the publication

2.3 Depth

Fredrich et al.(1988) find a centroid depth of 0 - 3 km based on inversion of long and short period waveforms. Boatwright and Choy (1992) analyse acceleration spectra from teleseismic data for the Marryat Creek event using a depth of 4.5 km, it is unclear what this depth is derived from. The GA_online catalogue and NSHA18 (Allen et al., 2018) report depths of 5 km but the justification for this depth is not stated. Barlow et al. (1986) report seismologically derived depths of 10 km and 19 km from different agencies, which are too deep to have caused a surface rupture for the moment of the earthquake. Uncertainty bounds are not reported for any depth estimates.

2.4 Foreshock / aftershocks

Large uncertainties due to poor instrumental density diminishes the ability to assess prior and post mainshock seismic activity in the region. The GA database includes two M_L 3.0 events between 1900 and the 1986 mainshock. The first is 50 km SW of the rupture in August 1983, and the other 85 km west in January 1985. Leonard (2008) suggests the national catalogue is complete for $M_L > 3.5$ from 1980, though the inclusion of these two events suggest the Marryat Creek area may have been complete for > 3.0 by 1983. The events are likely to be poorly located, given the ~35 km distance between the mainshock location and surface rupture. Many authors (Machette et al., 1993; McCue et al., 1987; etc) state that the area was aseismic prior to the mainshock, but given the lack of instrumentation available, the area may have experienced seismicity $M_L < 3.5$ prior to 1980 without being detected.

Aftershock activity for the mainshock is likewise affected by poor instrumentation. Five aftershocks M_L 3.0 - 3.3 were recorded in the seven days following the mainshock all poorly located (up to 100 km away from the rupture) with 13 other aftershocks recorded by the Alice Springs seismometer but not located (McCue et al., 1987). McCue (1990) suggests that the Alice Springs seismometer was capable of recorded seismic activity in the Marryat Creek area down to M_L 2.0. In July 1986 (4 months following the mainshock) a M_b 5.6 earthquake was recorded 8 km north of the GA epicentre (Allen et al., 2018), and ~35 km west of the rupture. McCue (1990) reports a “a few small aftershocks” from this event that aren’t published or recorded, followed by a cessation of seismicity in the region. A reconnaissance survey of the surface rupture was conducted prior to this event (Barlow et al., 1986), constraining the surface rupture to the March event rather than a combination of the March and July events which had similar magnitude values.

Eight temporary seismometers were deployed in 1990 (4 years after the mainshock) for 12 days with two events detected (Machette et al., 1993). The authors regard the first, located 14 km NW, as unrelated to the mainshock. The second, with a duration magnitude of 2 (Md) was located on the hanging-wall ~1 km west of the scarp at a depth of 1.1 ± 1.4 km. If this earthquake occurred on the seismogenic fault responsible for the MC_3 limb, it implies a fault dip of ~ 47°. No seismicity is recorded in the GA online catalogue within 25 km of the rupture since 1986.

3. Surface Rupture

3.1 Authors / map quality

The Marryat Creek surface rupture is one of the least accessible of all historic Australian ruptures, a 370 km drive south of Alice Springs or 1300 km north from Adelaide. The rupture occurred within the Anangu Pitjantjatjara Yankunytjatjara (APY) area of South Australia, making access dependant on permits. Despite the remoteness, detailed surveying was conducted along the length of rupture to characterise offset (Bowman and Barlow, 1991), aerial photography was obtained to help map the rupture, and multiple trenches were dug to characterise geometry and palaeoseismicity (Machette et al., 1993). The few published aerial images of the scarp (e.g. figure 8 Machette et al. (1993)) and 1:500 maps (Plate 2 (Machette et al., 1993)) show rupture complexity with duplexing ruptures, hanging-wall folding / cracking, and small < 20 m steps in rupture. This complexity is not captured in the published 1 : 10 000 and 1 : 50 000 maps of the rupture (e.g. (Bowman and Barlow, 1991; Machette et al., 1993)). The rupture trace from the GA Neotectonics Features database (Clark et al., 2012) and sections visible in Google and Bing satellite imagery do not align, due to datum transformation issues and simplification of fine-scale morphology in the original map.

3.2 Length and shape

The Marryat Creek scarp is highly arcuate in a concave direction (relative to the hanging-wall) with an 8 km distance between end points. The trace length of published maps of the rupture (Figure 7a) is between 13.8 -14.2 km (Bowman and Barlow, 1991; Machette et al., 1993). Bowman and Barlow (1991) describe lengths of 5.5 km for MC_1 and 7.5 km for the MC_3 (13 km total) where the mid-section of rupture (MC_2) is captured in the length of MC_1 (Figure 7b). A length of 13 km is used across publications describing the rupture (Barlow et al., 1986; Machette et al., 1993; McCue, 1990; McCue et al., 1987). Applying a criteria which simplifies ruptures to straight traces and defines distinct faults where mapped primary rupture has gaps/steps > 1 km and/or where strike changes by > 20° for distances > 1 km (e.g. (Quigley et al., 2017)) results in three faults with a total length of 13.6 km (Figure 7c) (explored in more detail in King et al. (2019) (in review)).

Figure 7d presents portions of the scarp where more than two vertical displacement measurements of greater than 0.2 m occur within a distance of 1 km (data from Bowman and Barlow (1991)). Applying cosmogenic erosion rates from lithologically and climatically analogous settings of Australia (0.3 – 5 m/Myr; Bierman and Caffee, 2002) suggests that 0.2 m of scarp height could be removed within 35 – 660 kyrs, leaving just 1 km of rupture length (i.e., 1 km of residual surface rupture with relief ≥ 0.2m) visible in the landscape. This suggests that the surface scarp may not persist within this landscape as a mappable scarp, unless recurrence intervals are < 0.5 to 1 Myr. Potential recurrence on this fault is limited by trenching results (Section 4) to > 130 ka (Machette et al., 1993). In this calculation we assume that the scarp is shallowly underlain by granitic bedrock and that the scarp erodes more rapidly than the surrounding terrain at rates commensurate with Bierman and Caffee (2002). We do not account for erosion rates of any duricrust which may overlie granitic bedrock or anthropogenically- and/or climatically-modulated variations in erosion rates.

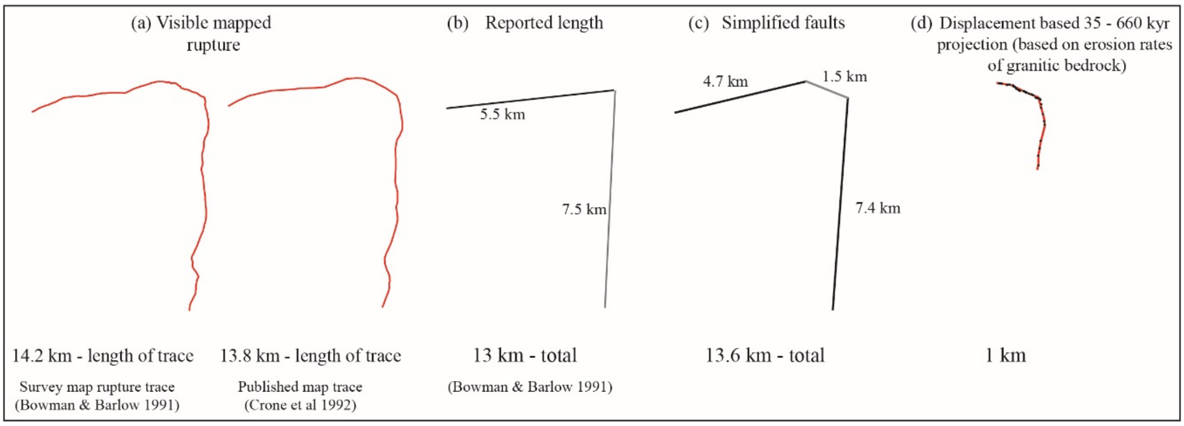

Figure 7: *Measures of length for the Marryat Creek surface rupture and underlying faults.*

3.3 Strike

The strike of the Marryat Creek rupture is highly variable due to the arcuate nature, with MC_1 trending 078°, MC_2 trending 117° and MC_3 trending 184° (Bowman and Barlow, 1991; Machette et al., 1993). A line drawn between end points trends 145°. The three main directions of surface rupture strike are shown relative to basement structural trends in *Figure 2*.

3.4 Dip

Cross sections across the rupture are shown in detailed survey maps presented in Bowman and Barlow (1991) including three with dip measurements (Figure 8). It is unclear if these measurements are from small trenches dug by the surveyor, from natural exposures of the rupture plane, or from calculations of dip based on vertical offset and heave. Machette et al. (1993) present two measurements of dip from trenches dug across the rupture (Figure 8). Together these dip measurements range from 36 – 60°, averaging 51° along MC_2 and MC_3. No dip measurements are recorded from MC_1.

Fredrich et al. (1988) prefer a dip of 35° ± 20 on a SW dipping plane from teleseismic body wave inversion while Barlow et al. (1986) prefer a dip of 67° on a south dipping plane based on p-wave first motions. These dips may be representative of an initial sub-event on MC_1 or MC_3 as described by P-wave first motions, followed by a mainshock on MC_2 as described by body-waves.

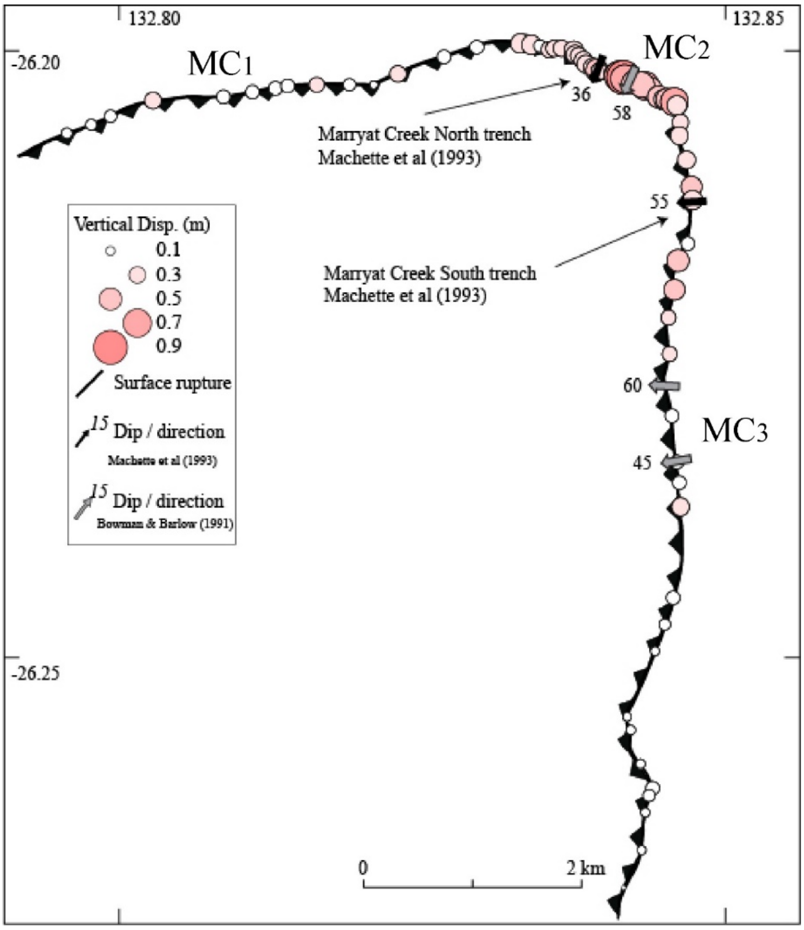

Figure 8 Map of the Marryat Creek scarp, vertical offset measurements, dip measurements and trench sites (digitised from Bowman and Barlow (1991) and Machette et al. (1993)).

3.5 Morphology

Machette et al. (1993) conducted their field mapping four years after the earthquake with much of the rupture and surface features still visible, though smaller details were destroyed by erosion and cattle. They describe the rupture as discrete with minor hanging-wall folding, or expressed as warping of the ground surface into a pressure ridge. The authors note en-echelon steps in the scarp separated by ramps or monoclines, though they do not mention the lengths, widths or directions of these features. An aerial photograph in McCue et al. (1987) shows ~10 - 20 m long duplexing discrete ruptures with an en-echelon, back-stepping morphology.

3.6 Lateral displacement

Barlow et al. (1986) published the first description of the surface rupture and note left-lateral slip on MC_1 and right-lateral slip on MC_3. Figure 3 of McCue et al. (1987) shows right-stepping transpression in discrete rupture on MC_3. Offsets of pre-existing animal and vehicle tracks were measured to estimate sinistral lateral offsets of 0.8 m on MC_1 (McCue et al., 1987) though these data are not presented in a map. A tree trunk was observed overlying part of MC_1, with a clear pre-event trunk impression on the ground showing 50 cm sinistral offset of the hanging-wall relative to foot-wall (sheet 10, (Bowman and Barlow, 1991)). No measurable lateral offsets are recorded for the MC_3 in any vehicle tracks or creeks that cross the scarp (Bowman and Barlow, 1991).

3.7 Displacement

Surveying along the rupture was conducted by the Australian Surveying and Land Information Group (now merged into Geoscience Australia) in April and August 1986. No uncertainties are specified for the surveying or levelling data, though Bowman and Barlow (1991) note that some error exists in vertical displacement measurements due to difficulties estimating scarp height in sandy terrain. Ten detailed profiles were collected, along dry creek beds where possible. Vertical displacement measurements and profiles shows that vertical displacement reaches a maximums of 0.5 - 0.9 m across 700 m along MC_2 and diminishes to < 0.25 m for the last 4 km of each limb.

Machette et al. (1993) appear to incorrectly reproduce some of the Bowman and Barlow (1991) displacement data due to conversion errors. This data is replicated in scaling relationships of Wesnousky (2008) and subsequent publications. We recommend referring to the data tables in Bowman and Barlow (1991), or King et al. (2019) (in review).

Due to the remote nature, no absolute offset measurements are available from resurveyed benchmarks, and no data regarding distributed deformation exist in the literature.

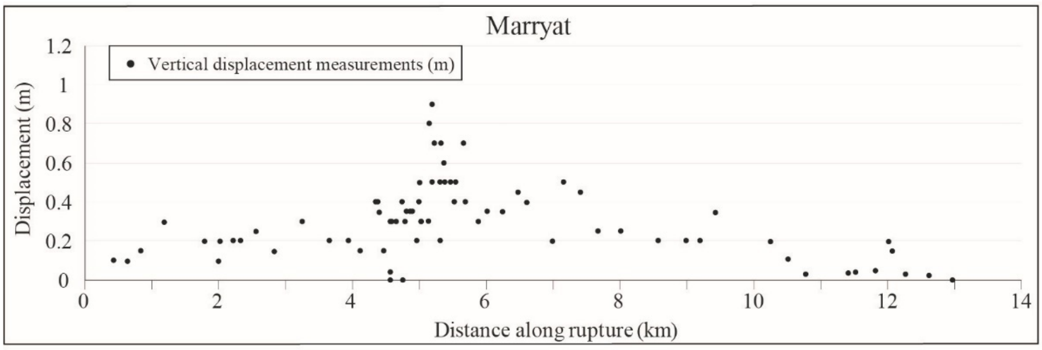

Figure 9 Vertical displacement measurements along the Marryat Creek scarp, digitised from Bowman and Barlow (1991). Methods described in Appendix A.

3.8 Environmental damage

Offset and length of the Marryat Creek surface rupture matches ESI IX – X (Michetti et al., 2007). Minimal fracturing is described in field studies of this earthquake, and none is shown on the maps. From descriptions and published images of the rupture, fracture lengths and widths are assigned ESI VII within a few meters of the surface rupture. Multiple authors describe grass and bushes killed from root tear on the hanging-wall at distances of 5 m (Bowman and Barlow, 1991; McCue et al., 1987). Rabbit warrens on the hanging-wall within ~10 m were observed to have collapsed, though warrens at similar distances on the foot-wall were intact (McCue et al., 1987). This vegetation and surface damage does not fall within the scope of the ESI-07 scale (Michetti et al., 2007). No authors report investigating bedrock outcrops in the area, so it is unknown whether rockfalls occurred or not. Similarly, no publications discuss hydrological anomalies in any nearby bores.

4. Paleoseismology

4.1 Summary

Machette et al. (1993) present detailed analysis of two trenches and eight samples taken for grain size analysis, uranium trend analysis and thermoluminescence dating. This work is also described in Crone et al. (1997).

4.2 Trenching

4.2.1. Identified units

Machette et al. (1993) includes comprehensive descriptions of units identified in two trenches (Marryat Creek South across MC_3 and Marryat Creek West across MC_2, *Figure 8*) and present a summary of exposed units alongside interpreted trench logs in Plate 1 of that report. The trenches are located on either side of the apex of rupture, in the area of maximum vertical offset. The western trench is ~10 m north of a dry creek bed, and the trench cuts across a small, low outcrop of "sheared granite" (granitic gneiss) on the hanging-wall. The southern trench is located just north of a very small dry tributary that eventually feeds into the Marryat Creek. Both trenches were 2 - 2.5 m deep with exposed bedrock at 0.3 and 1.25 m (west and south respectively). The authors interpret both trenches to show evidence of "ancient" (presumedly 580 - 520 Ma Petermann Orogeny) faulting, but no evidence of prior Cenozoic movement.

Bedrock in the MC_2 trench is described as 'fractured', 'sheared' and 'altered' granite. The fractured granite is described as having recognisable fabric and mineralogy, the sheared portions retain only some original granitic fabric and mineralogy, and the 'altered' granite is described as "extensively altered and sheared into light-greenish-gray clay". The altered granite is more abundant on the foot-wall, while the fresher granite is all on the hanging-wall.

Bedrock in the MC_3 trench is assumed to be originally basaltic and described as "altered rock (greenstone)", "sheared rock (greenstone)" and "fractured rock (greenstone)" with the same designation of 'fractured', 'altered' and 'sheared' as in the MC_2 trench granites. Unlike the MC_2 trench, the majority of 'fractured' greenstone (i.e. freshest) is found on the foot-wall of the modern rupture. The authors suggest that the extreme brecciation of the foot-wall bedrock in both trenches provides evidence of ancient faulting with "significant amount of differential movement" considering the width and extent of foot-wall alteration (>10's of meters). They identify that while some blocks of fresher granite are gradational into altered granite, some blocks with significantly different alteration levels are juxtaposed together along planes with the same geometry as the 1986 rupture.

Surficial sediments in the MC_2 trench are 15 - 30 cm thick and include 10 - 20 cm of eolian sand and 14 - 30 cm of poorly sorted fluvial gravel with 2 - 3 cm subangular to subrounded gravel clasts (Machette et al., 1993). The authors describe a weakly formed soil profile through the eolian sand and fluvial gravel and suggest that the soil profile is less developed on the hanging-wall of the rupture. Surficial sediments in the MC_3 trench are 0.7 - 1.2 m thick and include 10 - 20 cm of eolian sand, 0.05 - 0.75 m of poorly sorted sandy colluvial and fluvial gravel consisting of 1 - 2 cm clasts (up to 20 cm), and 0.75 - 1.25 m of poorly sorted gravel with clasts reflecting local bedrock. The authors identify a soil profile in the gravels that predates deposition of the eolian sands, but efforts to date the sediments using uranium trend analysis were unsuccessful, and no suitable material was found for radiocarbon dating. The authors instead use clay content, stratification and formation rates of calcium carbonate in the soil to estimate a 52 - 130 ka oldest depositional age for the quaternary sediments identified, with a preference for the older estimate.

4.2.2. Structural interpretations

In the MC_2 trench Machette et al. (1993) interpret basement geology to show that displacement in the 1986 earthquake was accommodated on a single fault plane that aligns to a pre-existing ancient fault. Extensional fractures on the hanging-wall are identified within 1.25 m of the rupture related to collapse of the hanging-wall block. The authors measure 46 - 47 cm of displacement across the base of surficial sediments, with additional offset from minor hanging-wall folding.

A similar set of structures are observed in the MC_3 trench, with displacement confined to a single 25 - 30 cm wide fault zone with the same orientation as gouge and calcium carbonate veins found in the heavily altered greenstone basement. No cracking or jointing is identified in this trench.

Displacements identified in the trenches match those measured at the surface, showing only historic offset of sediments overlying a bedrock fault structure presumably related to the Petermann orogeny (see Section 1.1).

4.3 Topography

McCue et al. (1987) note that the N-S rupture limb follows a linear topographic ‘mound’ for a few kilometres and suggest this may provide geomorphic evidence for a prior relief-generating event. However, Machette et al. (1993) consider the ridge to delineate differential erosion across resistant bedrock as it is not a persistent feature along the rupture, and their trench observations show no evidence of prior offset. Crone et al. (1997) suggest that the linear topographic high combined with a greater number of low sporadic bedrock outcrops on the hanging-wall compared to the foot-wall provide circumstantial evidence for prior Quaternary rupture. The distribution of bedrock on the hanging-wall compared to the foot-wall is consistent with differential erosion of bedrock affected by substantial Proterozoic fault movement and is not considered diagnostic of Quaternary rupture.

4.4 Slip rate

The strongest evidence for prior rupture comes from distinct boundaries between some semi-coherent basement blocks and heavily altered basement in trenches described by Machette et al. (1993). These semi-coherent blocks may have been faulted against altered material by prior Quaternary ruptures, though this evidence is circumstantial and may also relate to older faulting. Overall, there is no strong evidence to show any prior Quaternary rupture along the faults that hosted the 1986 Marryat Creek earthquake, and trenching shows an absence of rupture since 130 ka (the preferred depositional age described in Machette et al. (1993)).

The rupture is either the first Neotectonic event, or the recurrence interval is sufficiently long that all relief relating to prior event(s) was eroded prior to 130 ka. If recurrence is assumed, vertical relief generation rates are limited by very low bedrock erosion rates of < 5 m/Myr (Belton et al., 2004; Bierman and Caffee, 2002).

5. Summary

5.1 Surface rupture relationship to Geology

Machette et al. (1993) find evidence that at least across MC_2 and MC_3, rupture propagated along a fault presumably related to Neoproterozoic orogeny of the Musgrave Block. This is consistent with geophysical data which shows linear magnetic anomalies in this location with orientations colinear to both MC_2 and MC_3. The magnetic anomaly co-located with MC_1 is considered by some authors as the location of the Mann Fault (Aitken and Betts, 2009; Raimondo et al., 2010), a major Neoproterozoic crustal structure.

Large outcrops of gneiss within 1.5 km of the end of MC_1 and 4 km of MC_3 show three sets of dike, fault and foliation orientations (*Figure 2*). These outcrops are not shown on the Machette et al. (1993) geological map but are mapped on the 1 : 250,000 geological map of the area (Fairclough et al., 2011) and are visible in satellite imagery (*Figure 2*).

A NW-SE trending linear magnetic anomaly ~ 5.5 km SW of the surface rupture is coincident with the orientation of MC_2. This feature crosses MC_3 coincident with a distinct bend in the rupture trace. The trend of this feature is within 025° of the strike of both preferred focal mechanism planes (which have uncertainties of ± 020°) (Barlow et al., 1986; Fredrich et al., 1988). While there are no constraints on the depth, dip or dip direction of this linear magnetic anomaly, we hypothesise that it may represent the seismogenic fault as it’s strike and location are coincident with seismogenic data and fault geometry.

5.2 Surface rupture relationship to Seismology

Sinistral displacement on MC_1, dextral displacement on MC_3, and maximum vertical displacement on MC_2 support SW over NE movement of a hanging-wall block, consistent with two of the three published focal mechanisms. Trenching suggests that MC_2 is a through-going fault plane rather than potentially representing a near-surface linkage structure between MC_1 and MC_3 (e.g. as hypothesized for the 1968 Meckering surface rupture in Dentith et al. (2009)).

Due to poor instrumental coverage, epicentral locations and depths are highly uncertain and do not help to constrain rupture dynamics or fault geometry. A highly simplified cross section (*Figure 10*) across MC_1 and MC_3 using dip estimates based on surface measurements (corrected for apparent dip) and assuming two fault planes extend to depth, shows a conjugate intersection of structures at ~ 1.8 km depth. This fault intersection reaches 3 km depth (centroid depth derived by Fredrich et al. (1988)) approximately 5.5 km south west of the central section of rupture, coincident with the NE-SW trending magnetic anomaly described above.

Our preferred hypothesis to describe available seismological data (centroid depth and focal mechanisms), geophysical data (three sets of linear magnetic anomalies coincident with surface rupture orientations) and surface rupture measurements (maximum slip associated with the central section of ruptures, measured dips, and lateral kinematics) is: rupture initiating on a fault related to either MC_1 or MC_3 (or the intersection thereof) as described in P-wave first motion data (Barlow et al., 1986); rupture propagating onto a NW-SE orientated, SW dipping fault (e.g. MC_2) consistent with focal mechanisms from CMT and teleseismic body-waves (Ekström et al., 2012; Fredrich et al., 1988); a centroid of slip release at ~ 3 km depth ~ 5.5 km SW of MC_2 coincident with the intersection of the three prevailing planar bedrock structures; rupture propagating upwards along the SW dipping fault towards the surface rupture location of MC_2, and bilaterally across MC_1 and MC_3 resulting in lateral offsets along the limbs and maximum slip in the central area.

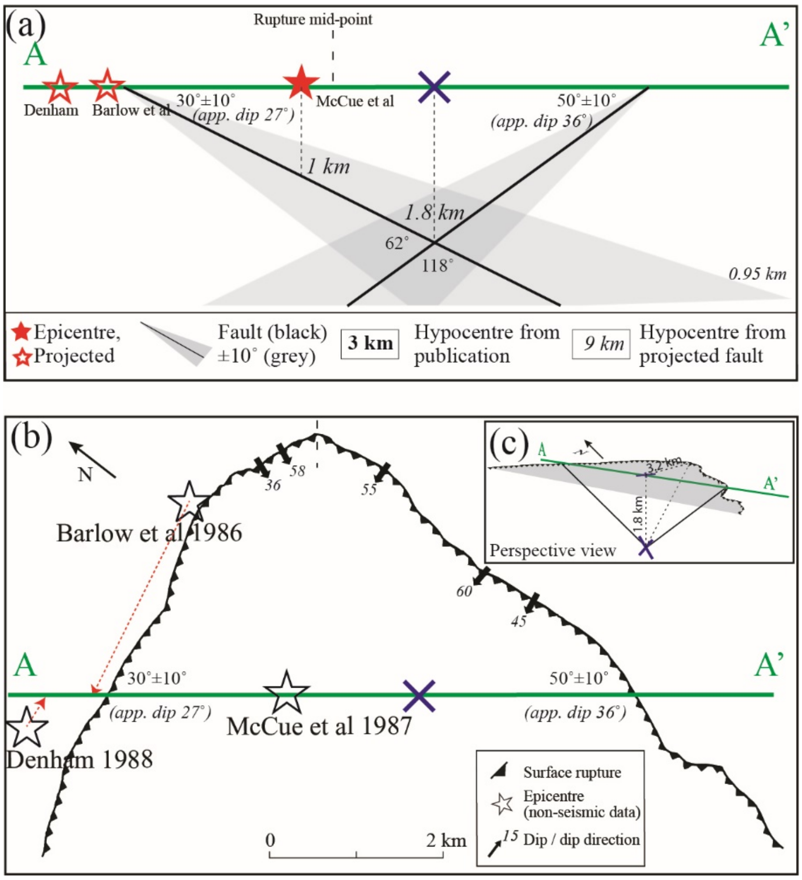

Figure 10: *Highly simplified cross section of the Marryat Creek scarp as two faults, using surface measurements of dips (± 10°, corrected to apparent dip), with published epicentres projected onto*

the cross section showing depth to simplified faults (italics), and published depths (bold). (c) shows a perspective view of the cross section (a) and map (b).

The number of distinct faults that are hypothesized to have ruptured in this earthquake (n=3), based on the criteria stated herein, is the highest estimate of multi-fault earthquakes at this magnitude (M_w 5.7) as ascertained from a recent global compilation (Figure 11).

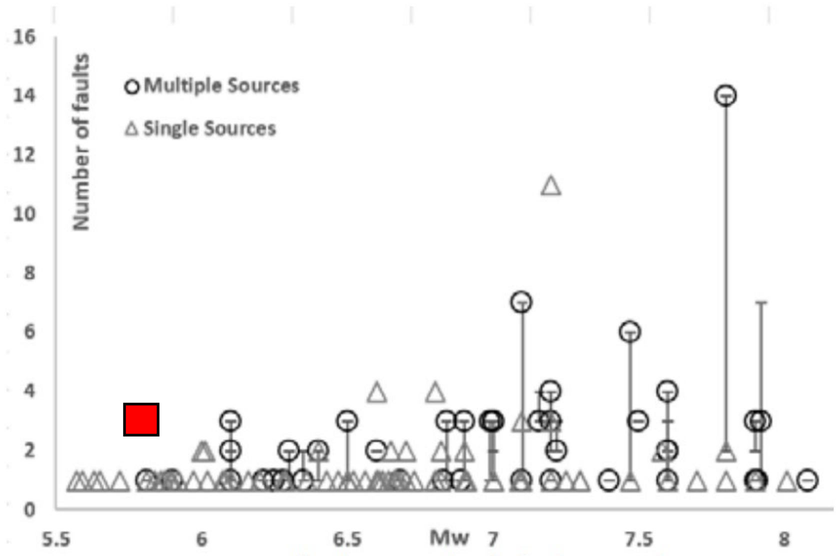

Figure 11 :From Fig. 5 of Quigley et al. (2017), Marryat Creek earthquake (red box) plotted against recent global compilation of number of geometrically-distinguished fault ruptures vs. Mw.

Acknowledgements

This research was funded by the Australian Research Council through Discovery Grant #DP170103350. T. King received funding through the Australian Government Research Training Program Scholarship. We would like to acknowledge the Antakirinja people of the Western Desert and APY lands in South Australia / Northern Territory, as the traditional custodians of the land on which this surface rupture occurred, and where the data described in this paper were collected. The authors declare no conflict of interest.

6. References

Aitken, A., Betts, P.G., 2009. Constraints on the Proterozoic supercontinent cycle from the structural evolution of the south-central Musgrave Province, central Australia. Precambrian Res. 168, 284–300. https://doi.org/10.1016/j.precamres.2008.10.006

Allen, T., Leonard, M., Ghasemi, H., Gibson, G., 2018. The 2018 National Seismic Hazard Assesment: Earthquake epicentre catalogue (GA Record 2018/30). Geoscience Australia, Commonwealth of Australia, Canberra, ACT. https://doi.org/http://dx.doi.org/10.11636/Record.2018.030

Barlow, B.C., Denham, D., Jones, T., McCue, K., 1986. The Musgrave Ranges earthquake of March 30, 1986. Trans. R. Soc. South Aust. 110, 187–189. https://doi.org/10.1126/science.97.2526.482-a

Belton, D.X., Brown, R.W., Kohn, B.P., Fink, D., Farley, K.A., 2004. Quantitative resolution of the debate over antiquity of the central Australian landscape: Implications for the tectonic and geomorphic stability of cratonic interiors. Earth Planet. Sci. Lett. 219, 21–34. https://doi.org/10.1016/S0012-821X(03)00705-2

Bierman, P.R., Caffee, M.W., 2002. Cosmogenic exposure and erosion history of Australian bedrock landforms. Bull. Geol. Soc. Am. 114, 787–803. https://doi.org/10.1130/0016-7606(2002)114<0787:CEAEHO>2.0.CO;2

Boatwright, J., Choy, G.L., 1992. Acceleration source spectra anticipated for large earthquakes in northeastern North America. Bull. Seismol. Soc. Am. 82, 660–682.

Bowman, J.R., Barlow, B.C., 1991. Surveys of the Fault Scarp of the 1986 Marryat Creek, South Australia, Earthquake (BMR Record 1991/109). Australian Seismological Centre, Bureau of Mineral Resources, Canberra, ACT. https://doi.org/http://pid.geoscience.gov.au/dataset/ga/14490

Cawood, P.A., Korsch, R.J., 2008. Assembling Australia: Proterozoic building of a continent. Precambrian Res. 166, 1–35. https://doi.org/10.1016/j.precamres.2008.08.006

Clark, D., McPherson, A., Van Dissen, R.J., 2012. Long-term behaviour of Australian stable continental region (SCR) faults. Tectonophysics 566–567, 1–30. https://doi.org/10.1016/j.tecto.2012.07.004

Crone, A.J., Machette, M.N., Bowman, J.R., 1997. Episodic nature of earthquake activity in stable continental regions revealed by palaeoseismicity studies of Australian and North American quaternary faults. Aust. J. Earth Sci. 44, 203–214. https://doi.org/10.1080/08120099708728304

Denham, D., 1988. Australian seismicity - the puzzle of the not-so-stable continent. Seismol. Res. Lett. 59, 235–240. https://doi.org/https://doi.org/10.1785/gssrl.59.4.235

Dentith, M., Clark, D., Featherstone, W.E., 2009. Aeromagnetic mapping of Precambrian geological structures that controlled the 1968 Meckering earthquake (Ms 6.8): Implications for intraplate seismicity in Western Australia. Tectonophysics 475, 544–553. https://doi.org/10.1016/j.tecto.2009.07.001

Edgoose, C.J., Scrimgeour, I.R., Close, D.F., 2004. Geology of the Musgrave Block, Northern Territory (NTGS Report 15). Northern Territory Geological Survey, Darwin, Australia.

Ekström, G., Nettles, M., Dziewoński, A.M., 2012. The global CMT project 2004-2010: Centroid-moment tensors for 13,017 earthquakes. Phys. Earth Planet. Inter. 200–201, 1–9. https://doi.org/10.1016/j.pepi.2012.04.002

Fairclough, M.C., Sprigg, R.C., Wilson, B., Coats, R.P., 2011. Alberga 1:250 000 Geological Map, Digital Edition. Geological Survey of South Australia, Adelaide, Australia.

Fredrich, J., Mccaffrey, R., Denham, D., 1988. Source parameters of seven large Australian earthquakes determined by body waveform inversion. Geophys. J. 95, 1–13. https://doi.org/https://doi.org/10.1111/j.1365-246X.1988.tb00446.x

Hand, M., Sandiford, M., 1999. Intraplate deformation in central Australia, the link between subsidence and fault reactivation. Tectonophysics 305, 121–140. https://doi.org/10.1016/S0040-1951(99)00009-8

King, T.R., Quigley, M.C., Clark, D., 2019. Surface-rupturing historical earthquakes in Australia and their environmental effects: new insights from re-analyses of observational data. Geosciences.

Korsch, R.J., Goleby, B.R., Leven, J.H., Drummond, B.J., 1998. Crustal architecture of central Australia based on deep seismic reflection profiling. Tectonophysics 288, 57–69. https://doi.org/10.1016/S0040-1951(97)00283-7

Lambeck, K., Burgess, G., 1992. Deep crustal structure of the musgrave block, central australia: Results from teleseismic travel-time anomalies. Aust. J. Earth Sci. 39, 1–19. https://doi.org/10.1080/08120099208727996

Leonard, M., 2008. One hundred years of earthquake recording in Australia. Bull. Seismol. Soc. Am. 98, 1458–1470. https://doi.org/10.1785/0120050193

Machette, M.. M.N., Crone, A.. A.J., Bowman, J.R., Bowman, R.J., Bowman, J.R., 1993. Geologic investigations of the 1986 Marryat Creek, Australia, earthquake: implications for paleoseismicity in stable continental regions (USGS Bulletin 2032-B). Washington, USA. https://doi.org/https://doi.org/10.3133/b2032B

McCue, K., 1990. Australia's large earthquakes and Recent fault scarps. J. Struct. Geol. 12, 761–766. https://doi.org/10.1016/0191-8141(90)90087-F

McCue, K., Jones, T., Michael-Leiba, M., Barlow, B.C., Denham, D., Gibson, G., 1987. Another chip off the old Australian block. Eos, Trans. Am. Geophys. Union 68, 609. https://doi.org/10.1029/eo068i026p00609

Michetti, A.M., Esposito, E., Guerrieri, L., Porfido, S., Serva, L., Tatevossian, R.E., Vittori, E., Audemard M., F.A., Azuma, T., Clague, J., Comerci, V., Gurpinar, A., McCalpin, J.P., Mohammadioun, B., Morner, N.A., Ota, Y., Roghozhin, E., 2007. Intensity Scale ESI 2007, Memorie Descrittive della Carta Geologica d'Italia, Special Volume 74. APAT, Rome 2007.

Neumann, N.L., 2013. Yilgarn Craton – Officer Basin – Musgrave Province Seismic and MT Workshop (GA Record 2013/28). Geoscience Australia, Commonwealth of Australia, Canberra, ACT. https://doi.org/http://pid.geoscience.gov.au/dataset/ga/76664

Quigley, M.C., Mohammadi, H., Duffy, B.G., 2017. Multi-fault earthquakes with kinematic and geometric rupture complexity : how common ? INQUA Focus Group Earthquake Geology and Seismic Hazards.

Raimondo, T., Collins, A.S., Hand, M., Walker-Hallam, A., Smithies, R.H., Evins, P.M., Howard, H.M., 2010. The anatomy of a deep intracontinental orogen. Tectonics 29. https://doi.org/10.1029/2009TC002504

Stewart, A.J., 1995. Western extension of the Woodroffe Thrust, Musgrave Block, central Australia. AGSO J. Aust. Geol. Geophys. 16, 147–153.

Wade, B.P., Kelsey, D.E., Hand, M., Barovich, K.M., 2008. The Musgrave Province: Stitching north, west and south Australia. Precambrian Res. 166, 370–386. https://doi.org/10.1016/j.precamres.2007.05.007

Wesnousky, S.G., 2008. Displacement and geometrical characteristics of earthquake surface ruptures: Issues and implications for seismic-hazard analysis and the process of earthquake rupture. Bull. Seismol. Soc. Am. 98, 1609–1632. https://doi.org/10.1785/0120070111

Wex, S., Mancktelow, N.S., Camacho, A., Pennacchioni, G., 2019. Interplay between seismic fracture and aseismic creep in the Woodroffe Thrust, central Australia – Inferences for the rheology of relatively dry continental mid-crustal levels. Tectonophysics 758, 55–72. https://doi.org/10.1016/j.tecto.2018.10.024

Appendix A

Methods for digitising vertical displacement data and benchmark data

Vertical offset measurements are presented in Tables 1 – 4 of Bowman and Barlow (1991) alongside decimal and UTM coordinates. These tables were copied from PDF into excel and thoroughly checked for copy errors. The CSV of decimal degrees and vertical displacements was then imported into GIS and checked against the surface rupture trace. A short script[2] was used in QGIS attribute manager field calculator to extract the distance of each vertical offset measurement along the surface rupture trace. The shape file was extracted into a final CSV with x-y coordinates, vertical offset measurements, and distance along fault data.

Three dip measurements are shown in sketches on survey plates of Bowman and Barlow (1991). These were digitised based on the location of the closest survey point as previously imported from the vertical offset tables. Two dip measurements from trenches described in Machette et al. (1993) were digitised directly from trench sites identifiable on high resolution satellite imagery, cross-referenced to the trench location shown on Plate 2 of Machette et al. (1993).

[2] line_locate_point(geometry:=geometry(get_feature('Line', 'id', '1')), point:=$geometry)